A Reactive Collision Avoidance Algorithm for Vehicles with Underactuated Dynamics

Martin S. Wiig[1,2], Kristin Y. Pettersen[1,2] and Thomas R. Krogstad[2]

Abstract— This paper presents a reactive collision avoidance algorithm, which avoids both static and moving obstacles by keeping a constant avoidance angle between the vehicle velocity vector and the obstacle. In particular, we consider marine vehicles with underactuated sway dynamics, which cannot be directly controlled. This gives an underactuated component in the vehicle velocity, which the proposed algorithm is designed to compensate for. The algorithm furthermore compensates for the obstacle velocity. Conditions are derived under which the sway movement is bounded and collision avoidance is mathematically proved. The theoretical results are supported by simulations. The proposed algorithm makes only limited sensing requirements on the vehicle, is intuitive and suitable for a wide range of vehicles. This includes vehicles with heavy forward acceleration constraints, which is demonstrated by applying the algorithm to a vehicle with constant surge speed.

I. INTRODUCTION

To operate safely in dynamic environments, unmanned vehicles should be able to avoid collisions with both obstacles and other vehicles. The collision avoidance (CA) problem becomes particularly challenging for underactuated vehicles, as not all degrees of freedom (DOF) can be independently controlled. In particular, underactuation generally introduces second-order nonholonomic constraints, which makes it necessary to take the underactuated dynamics into consideration [1]. Hence, it is not sufficient to consider a purely kinematic model for motion planning and control of underactuated vehicles.

In this paper we consider marine vehicles moving in the horizontal plane, with underactuated dynamics in the sideways (sway) direction. Marine vehicles often have a large mass, making substantial changes in the forward (surge) speed undesirable. A CA algorithm for marine vehicles should thus take into account the forward acceleration limitations of the vehicle, which we do in this paper by considering a vehicle keeping a constant forward speed.

Surveys of recent results in CA algorithms can be found in [2]–[4]. The different approaches can generally be divided into motion planning algorithms and reactive algorithms. Motion planning algorithms can be intractable for vehicles with limited processing power, particularly in uncertain and dynamic environments requiring high planning frequency.

[1]Centre for Autonomous Marine Operations and Systems (NTNU AMOS), Department of Engineering Cybernetics, Norwegian University of Science and Technology, 7491 Trondheim, Norway. `Martin.Wiig@itk.ntnu.no`

[2]Norwegian Defence Research Establishment (FFI), P.O. Box 25, N-2027 Kjeller, Norway.

There is therefore a need for reactive algorithms, which also can provide valuable redundancy to collision avoidance systems based on motion planning.

A much used approach to reactive CA is the artificial potential field method [5], which is simple to implement and scales well with environment complexity. There are, however, some stability issues with the approach [6], which is avoided in the related vector field histogram algorithm [7]. Still, vehicle dynamics is not included in the analysis of the vehicle behavior, and only static obstacles are considered.

The dynamic window algorithm [8] finds provably safe control inputs for vehicles with first-order nonholonomic constraints. It is extended to include the second-order nonholonomic constraints resulting from the underactuation of marine vehicles in [9]. The approach works well in complex environments, but only considers static obstacles.

Moving obstacles are inherently considered in the velocity obstacles (VO) approach [10], which generates a set of safe velocities even in a crowded environment. In [11], the approach is extended to include COLREGs, the maritime rules of the road. The approach assumes, however, that the vehicle is fully actuated with unbounded acceleration.

The acceleration VO approach [12] includes acceleration constraints in a fully actuated vehicle. It can be used on a vehicle with unicycle-type constraints as well, but becomes restrictive if the forward acceleration capability of the vehicle is limited. The generalized VO [13] represents the VO in terms of control input, and can thus be used on underactuated systems with second-order nonholonomic constraints. It can, however, be computationally expensive.

In [14], input-output linearization is used to reduce the kinematics and dynamics of a unicycle to a set of double integrators, which is used by a CA algorithm to provably avoid moving obstacles. However, like the acceleration VO, the approach is restrictive for vehicles with a limited forward acceleration capability.

The reactive CA algorithm proposed by [15] makes the vehicle circumvent moving obstacles. It is mathematically proved that a marine vehicle with underactuation in sway is able to execute a successful CA maneuver, while adhering to COLREGs. Set-based theory is used to switch between CA and path following. However, no analytical bound is found for the obstacle distance at which the switch should occur.

In [16], a CA algorithm for unicycles is presented. The algorithm makes the vehicle keep a constant avoidance angle to the obstacle, and it is proved that obstacles moving at a constant velocity are avoided. The forward acceleration can be significant during the maneuver, however, which

makes the algorithm less suitable for vehicles with forward acceleration constraints. To accommodate such vehicles, the algorithm proposed in [17] extends the approach to vehicles with a constant forward speed. However, only vehicle kinematics are included in the analysis.

The main contribution of this paper is an extension of the CA algorithm presented in [17] to marine vehicles. The marine vehicle has sway dynamics, which can make the vehicle glide sideways into the obstacle. Moreover, the sway dynamics are underactuated and can therefore only be indirectly controlled through the actuated states. Hence we can no longer use a purely kinematic model, like we could in [17], but have to include the sway dynamics as well.

We will show that the sway dynamics is bounded during the CA maneuver. Furthermore, we derive conditions under which it is mathematically proved that both static and moving obstacles can be safely avoided. This includes a lower bound on the minimum distance between the vehicle and the obstacle, at which the vehicle should enter CA mode.

The proposed algorithm is applied to a vehicle with constant forward speed, thus accommodating vehicles with heavy forward acceleration constraints. However, it can also be applied to vehicles without such restrictions, which gives flexibility in the design of the desired surge trajectory. The algorithm we present is intuitive, has a low computational complexity and makes only limited sensing requirements on the vehicle.

The remainder of this paper is organized as follows. Section II describes the vehicle and obstacle models, the sensing model and the control objective of the system. Section III gives a description of the course controller, as well as of the target reaching guidance law employed when the vehicle is not in CA mode. Section IV describes the CA algorithm. Mathematical proofs of bounded sway and a safe CA maneuver are given in Section V, and the theory is supported by simulations in Section VI. Finally, some concluding remarks are given in Section VII.

II. SYSTEM DESCRIPTION

A. Vehicle model

We consider a marine vehicle moving in 3 DOF, which is modeled as [18]:

$$\dot{x} = u\cos(\psi) - v\sin(\psi), \tag{1a}$$
$$\dot{y} = u\sin(\psi) + v\cos(\psi), \tag{1b}$$
$$\dot{\psi} = r, \tag{1c}$$
$$\dot{v} = Xr + Yv. \tag{1d}$$

The vehicle's Cartesian coordinates are denoted x and y, while the surge (forward) and sway (sideways) speeds are denoted u and v, respectively. Furthermore, ψ and r denote the yaw and yaw rate. The vehicle position is defined as $\boldsymbol{p} \triangleq [x, y]^T$. The terms X and Y are defined as

$$X \triangleq S_X u + C_X, \tag{2}$$
$$Y \triangleq S_Y u + C_Y \tag{3}$$

where S_X, C_X, S_Y and C_Y are constant model parameters, which may be positive or negative, derived from the mass and damping coefficients of the vehicle [18]. The vehicle is directly actuated in u and r, but has no actuation in v. Hence, the sway dynamics has to be included in the model, while the surge and yaw dynamics can be removed by Assumption 1.

Assumption 1: The surge speed u and yaw rate r are perfectly controlled, and can thus be considered as virtual control inputs. Furthermore, u is positive and constant.

Assumption 2: The Y term satisfies $Y < 0$.
Assumption 2 ensures that the system is damped and nominally stable in sway, which is the case for most vehicles.

In order to control the direction of the vehicle's velocity vector, we will control the vehicle course instead of its heading ψ. To this end, we make the coordinate transformation $[x, y, \psi]^T \rightarrow [x, y, \chi]^T$, where $\chi \triangleq \psi + \operatorname{atan2}(v, u)$. The model in the new coordinates is

$$\dot{x} = U\cos(\chi), \tag{4a}$$
$$\dot{y} = U\sin(\chi), \tag{4b}$$
$$\dot{\chi} = r_\chi, \tag{4c}$$
$$\dot{v} = \frac{U^2}{Xu + U^2}\left(Xr_\chi + Yv\right), \tag{4d}$$

where $U \triangleq \sqrt{u^2 + v^2}$ and

$$r_\chi \triangleq \frac{\left(Xu + U^2\right)r + Yuv}{U^2}. \tag{5}$$

The following assumption is required to ensure that (4d) is well defined [19]:

Assumption 3: The X term satisfies $X + u > 0$.
Remark 1: Assumption 3 ensures that a change in the heading ψ always results in a change in the course χ, and is satisfied for most vessels.

B. Obstacle model

We consider a single obstacle. Since it can be difficult to estimate the dynamic parameters of the obstacle, it is modeled as a unicycle-type vehicle:

$$\dot{x}_{\mathrm{o}} = U_{\mathrm{o}}\cos(\chi_{\mathrm{o}}), \tag{6a}$$
$$\dot{y}_{\mathrm{o}} = U_{\mathrm{o}}\sin(\chi_{\mathrm{o}}), \tag{6b}$$
$$\dot{\chi}_{\mathrm{o}} = r_o, \tag{6c}$$
$$\dot{u}_{\mathrm{o}} = a_{\mathrm{o}}, \tag{6d}$$

where x_{o} and y_{o} are the Cartesian coordinates of the obstacle, U_{o} and a_{o} are the forward speed and acceleration, and χ_{o} and r_o are the obstacle course and course rate, respectively. The obstacle velocity vector is denoted $\boldsymbol{v}_o \triangleq [\dot{x}_{\mathrm{o}}, \dot{y}_{\mathrm{o}}]^T$.

Assumption 4: The obstacle is modeled as a moving circular domain D of radius R with center at $[x_{\mathrm{o}}, y_{\mathrm{o}}]^T$.

Remark 2: The proposed collision avoidance algorithm can also be applied to non-circular obstacles, which is demonstrated in a simulation in Section VI.

Assumption 5: The obstacle forward speed U_{o} lies in the interval $U_{\mathrm{o}} \in [0, U_{\mathrm{o,max}}]$, where

$$U_{\mathrm{o,max}} < \begin{cases} 2\sqrt{-X^2 - Xu} & -u < X \le -\frac{u}{2} \\ u & -\frac{u}{2} < X. \end{cases} \tag{7}$$

Remark 3: The bound $U_{o,\max} < u$ follows from the fact that the vehicle circles around the obstacle when in CA mode. The bound $U_{o,\max} < 2\sqrt{-X^2 - Xu}$ restricts $U_{o,\max}$ further if a large sway motion towards the obstacle is induced by turning away from it. This follows from the mathematical analysis in Section V.

Assumption 6: The obstacle forward acceleration a_o and course rate r_o are bounded by

$$a_o \in [-a_{o,\max}, a_{o,\max}], \tag{8}$$

$$r_o \in [-r_{o,\max}, r_{o,\max}], \tag{9}$$

where $a_{o,\max} \geq 0$ and $r_{o,\max} \geq 0$ are constant parameters.

C. Sensing requirements

In this section we state the obstacle measurements required of the vehicle to implement the proposed CA algorithm. First, it is required to sense the distance d between the vehicle position $\boldsymbol{p}$ and the obstacle. The obstacle velocity vector $\boldsymbol{v}_o$ is also required. Finally, the vehicle must be able to measure the angles $\alpha^{(1)}$ and $\alpha^{(2)}$ defining the vision cone $\mathcal{V}$ from the vehicle to the obstacle, as shown in Figure 1.
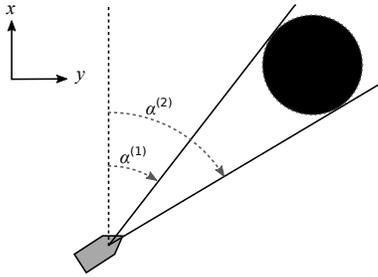

Fig. 1. The vision cone $\mathcal{V}$ from the vehicle to the obstacle.

D. Control objective

The control system and the CA algorithm should make the vehicle reach a target position $\boldsymbol{p}_t = [x_t, y_t]^T$ while keeping a minimum safety distance, d_{safe}, to the obstacle,

$$d(t) \geq d_{\text{safe}} > 0 \quad \forall t \geq 0. \tag{10}$$

Furthermore, the sway velocity of the vehicle is required to be bounded,

$$|v(t)| < v_{\text{sup}} \quad \forall t \geq 0, \tag{11}$$

where $v_{\text{sup}} > 0$ is a constant design parameter.

Assumption 7: The initial sway speed satisfies $|v(0)| < v_{\text{sup}}$.

III. CONTROL SYSTEM

The control system has two modes, guidance mode and CA mode, which is switched between according to the rule we give in Section IV-B. The desired course during guidance mode is given by a pure pursuit guidance law described in Section III-B, while in CA mode it is given by the CA algorithm presented in Section IV.

A. Course controller

To obtain exponential course convergence, the desired course reference χ_d is tracked using the controller

$$r_\chi = \dot{\chi}_d - k_\chi \tilde{\chi}, \tag{12}$$

where k_χ is a positive control gain. The course error $\tilde{\chi} \triangleq \chi - \chi_d$ is defined to lie in the interval $\tilde{\chi} \in (-\pi, \pi]$, to ensure that the vehicle always makes the shortest turn towards χ_d. From (4c) it is clear that (12) provides exponential stability of the course error dynamics. We find the corresponding yaw rate by inserting (12) into (5):

$$r = \frac{U^2 r_\chi - Yuv}{Xu + U^2}, \tag{13}$$

which is ensured to be well defined by Assumption 3.

B. Guidance law

When the control system is in guidance mode, the course reference is given by a pure pursuit guidance law [20]:

$$\chi_{dg} \triangleq \text{atan2}\,(y_t - y, x_t - x), \tag{14}$$

where $\chi_{dg} \in [0, 2\pi)$ is the course reference. Note that under this guidance law, $\dot{\chi}_{dg} = 0$ when $\tilde{\chi} = 0$, which simplifies the analysis in Section V.

IV. COLLISION AVOIDANCE ALGORITHM

This section describes the proposed CA algorithm. While the algorithm in [17] was based on the kinematics of unicycle-type nonholonomic vehicles, the second-order non-holonomic constraint given by the underactuation makes it necessary to include the sway dynamics. In particular, the total vehicle speed contains a time-varying component from sway, which has to be considered in the analysis in Section V. While the algorithm in [17] provided a desired heading, we will in this paper make the CA algorithm steer the vehicle course instead. We will show that it is thus possible to handle the sway dynamics and guarantee collision avoidance.

A. Desired vehicle course

Two velocity vectors, $\boldsymbol{v}_\beta^{(1)}$ and $\boldsymbol{v}_\beta^{(2)}$, with a constant avoidance angle α_o to the vision cone $\mathcal{V}$ (Figure 1) are created by extending $\mathcal{V}$ by α_o as shown in Figure 2. The direction of $\boldsymbol{v}_\beta^{(1)}$ and $\boldsymbol{v}_\beta^{(2)}$ are denoted $\beta^{(1)}$ and $\beta^{(2)}$,

$$\boldsymbol{v}_\beta^{(j)} \triangleq u_\beta^{(j)} \left[\cos(\beta^{(j)}), \sin(\beta^{(j)})\right], \quad j = \{1, 2\}, \tag{15}$$

where $u_\beta^{(j)}$ will be defined later.

To avoid a moving obstacle, the CA algorithm will make the vehicle keep the velocity $\boldsymbol{v}_\beta^{(j)}$ in a non-rotating coordinate frame moving with the obstacle velocity $\boldsymbol{v}_o$. This is achieved by compensating the extended vision cone for $\boldsymbol{v}_o$, thus creating a compensated vision cone $\mathcal{V}_c$ as illustrated in Figure 3. The sides of $\mathcal{V}_c$ are defined by the vectors

$$\boldsymbol{v}_{ca}^{(j)} \triangleq \boldsymbol{v}_\beta^{(j)} + \boldsymbol{v}_o, \quad j = \{1, 2\}, \tag{16}$$

which are the candidates for the desired vehicle velocity in CA mode. To ensure that the directions of $\boldsymbol{v}_{ca}^{(j)}$ are safe at the current vehicle speed U, their length is set to $||\boldsymbol{v}_{ca}^{(j)}|| \triangleq U$.

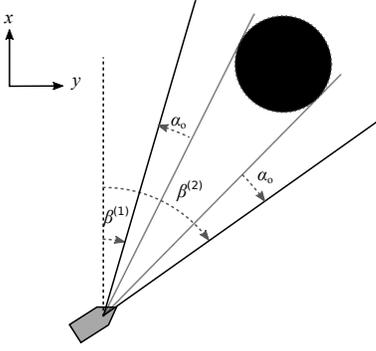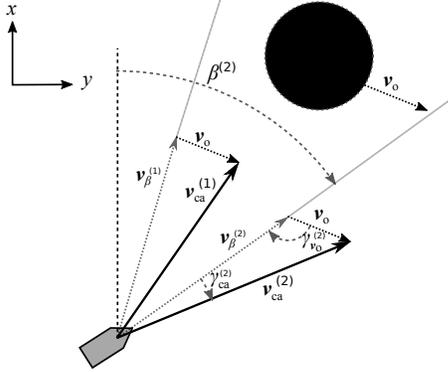Fig. 2. The extended vision cone from the vehicle to the obstacle.

Fig. 3. The desired velocity vector candidates $\boldsymbol{v}_{\text{ca}}^{(1)}$ and $\boldsymbol{v}_{\text{ca}}^{(2)}$, which define the sides of the compensated vision cone $\mathcal{V}_{\text{c}}$.

The angle $\gamma_{\text{ca}}^{(j)}$ between $\boldsymbol{v}_{\beta}^{(j)}$ and $\boldsymbol{v}_{\text{ca}}^{(j)}$ is designed to compensate for the obstacle velocity, and is found as

$$\gamma_{\text{ca}}^{(j)} = \sin^{-1}\left(\frac{U_{\text{o}}\sin(\gamma_{\boldsymbol{v}_o}^{(j)})}{U}\right), \quad j = \{1, 2\}, \quad (17)$$

where $\gamma_{\boldsymbol{v}_o}^{(j)}$ can be found from geometry as

$$\gamma_{\boldsymbol{v}_o}^{(j)} = \pi - (\chi_{\text{o}} - \beta^{(j)}), \quad j = \{1, 2\}. \quad (18)$$

The candidates for desired vehicle course in CA mode are then defined as

$$\chi_{\text{dca}}^{(j)} \triangleq \beta^{(j)} + \gamma_{\text{ca}}^{(j)}, \quad j = \{1, 2\}, \quad (19)$$

Section IV-C provides a rule for choosing between these two candidates.

B. Switching rule

We define that the vehicle enters collision avoidance mode at a time t_1 if

$$\chi_{\text{dg}}(t_1) \in \mathcal{V}_{\text{c}}(t_1), \quad (20)$$

$$d(t_1) \leq d_{\text{switch}}, \quad (21)$$

where $d_{\text{switch}} > d_{\text{safe}}$ is a design parameter. Nominal guidance towards the target will resume at a time t_2 when $\chi_{\text{dg}}(t_2)$ moves outside $\mathcal{V}_{\text{c}}(t_2)$:

$$\chi_{\text{dg}}(t_2) \notin \mathcal{V}_{\text{c}}(t_2). \quad (22)$$

C. Turning direction

The proposed CA algorithm (19) provides two candidates for the desired course in order to avoid collision. We will use this flexibility to make the vehicle seek to move behind the obstacle, which often is the safest course of action. In particular, we choose the following direction parameter j when the vehicle enters CA mode at a time t_1:

$$j = \begin{cases} \arg\max_{j=1,2} & |\chi_{\text{o}}(t_1) - \chi_{\text{dca}}^{(j)}(t_1)|, \quad d(t_1) = d_{\text{switch}}, \\ \arg\min_{j=1,2} & |\chi(t_1) - \chi_{\text{dca}}^{(j)}(t_1)|, \quad d(t_1) < d_{\text{switch}}. \end{cases} \quad (23)$$

When $d(t_1) = d_{\text{switch}}$ this maximizes the difference between the obstacle course and $\chi_{\text{dca}}^{(j)}$. However, if the obstacle is closer than d_{switch} when the vehicle enters CA mode, the vehicle will make the shortest turn towards a safe direction. This can for instance happen if a nearby obstacle turns so that the current vehicle course becomes unsafe.

Remark 4: The algorithm avoids collisions regardless of the method used to choose j when $d(t_1) = d_{\text{switch}}$.

V. MATHEMATICAL ANALYSIS

This section presents a mathematical analysis of the vehicle (4) when the CA law given in Section IV is used in combination with the course controller and guidance law in Section III. In particular, we derive conditions on the course control gain k_χ, the safety distance d_{safe} and the switching distance d_{switch} which ensures that a circular obstacle moving with a time-varying velocity can be safely avoided.

When the course rate $r_\chi \neq 0$, a sway motion v is induced by (4d). To prevent the vehicle from being driven into the obstacle by the sway motion, we need to bound v, which is done in the next two lemmas.

Lemma 1: Consider a vehicle modeled by (4). Suppose that the course rate r_χ is dependent on the sway motion v in such a way that for $v = v_{\text{sup}}$,

$$|r_\chi(\pm v_{\text{sup}})| < \frac{|Y|}{|X|}v_{\text{sup}}. \quad (24)$$

Then, if $|v(0)| < v_{\text{sup}}$, the solutions of v are bounded by

$$|v(t)| < v_{\text{sup}} \quad \forall t \geq 0. \quad (25)$$

Proof: Consider the Lyapunov function

$$V = \tfrac{1}{2}v^2. \quad (26)$$

The time derivative of V along the solutions of (4d) is

$$\dot{V} = \frac{U^2}{U^2 + Xu}\left(Xvr_\chi + Yv^2\right). \quad (27)$$

When Assumption 2 holds, (27) is bounded by

$$\dot{V} \leq \frac{U^2}{U^2 + Xu}\left(|X||v||r_\chi(v)| - |Y|v^2\right). \quad (28)$$

Let the set Ω_v be defined as

$$\Omega_v \triangleq \{v \in \mathbb{R} \mid V \leq \tfrac{1}{2}v_{\text{sup}}^2\}, \quad (29)$$

which is a level set of V with $v = v_{\text{sup}}$ on the boundary. Equation (24) ensures that $\dot{V} \leq 0$ on the boundary of Ω_v. It follows that any solution of v starting in the set Ω_v cannot

leave it. Hence, if $|v(0)| \leq v_{\text{sup}}$, then $|v(t)| \leq v_{\text{sup}} \; \forall t \geq 0$. ∎

Before stating the next lemma, we define the following term for conciseness:

$$F_{kd} \triangleq |Y| v_{\text{sup}} \left(\frac{1}{|X|} - 2 \frac{v_{\text{sup}} U_{\text{o,max}}}{U_{\text{d,sup}} \left(Xu + U_{\text{sup}}^2 \right)} \right) \qquad (30)$$
$$- r_{\text{o,max}} \frac{U_{\text{o,max}}}{U_{\text{sup}}} - \frac{a_{\text{o,max}}}{U_{\text{d,sup}}},$$

where $U_{\text{sup}} \triangleq \sqrt{u^2 + v_{\text{sup}}^2}$ and $U_{\text{d,sup}} \triangleq \sqrt{U_{\text{sup}}^2 - U_{\text{o,max}}^2}$.

Remark 5: Since U_{sup} increases with increasing v_{sup}, it is always possible to choose a v_{sup} large enough to ensure a positive value of F_{kd}.

We also introduce the design parameter $\sigma \in (0,1)$, which is used to prioritize between the control gain k_χ and the safety distance d_{safe}. A high value of σ will give priority to a high k_χ, while a low value of σ prioritizes a low d_{safe}.

Lemma 2: Consider a vehicle modeled by (4), controlled by the course controller (12) - (13), with a desired course given by the CA law (19). Let $\sigma \in (0,1)$, and assume that the distance between the vehicle and the obstacle satisfies $d(t) > d_{\text{safe}} \; \forall t \geq 0$. If Assumptions 1-6 hold, the course control gain k_χ satisfies

$$k_\chi \leq \frac{\sigma}{\pi} F_{kd}, \qquad (31)$$

the safety distance d_{safe} satisfies

$$d_{\text{safe}} \geq \frac{(U_{\text{sup}} + U_{\text{o,max}})^2}{U_{\text{sup}}} \frac{1}{(1 - \sigma) F_{kd}}, \qquad (32)$$

and the initial sway speed satisfies $|v(0)| \leq v_{\text{sup}}$, then

$$|v(t)| \leq v_{\text{sup}} \quad \forall t \geq 0 \qquad (33)$$

Proof: We prove Lemma 2 by finding an upper bound on r_χ for a given v_{sup}. Lemma 1 is then applied by inserting the upper bound into (24), and solving for k_χ and d_{safe} to obtain (31) and (32).

It can be shown that the time derivative of $\chi_{\text{dca}}^{(j)}$ is

$$\dot{\chi}_{\text{dca}}^{(j)} = \dot{\beta}^{(j)} + \frac{1}{\sqrt{U^2 - U_o^2 \sin^2(\gamma_{v_o}^{(j)})}} \qquad (34)$$
$$\cdot \left[\sin(\gamma_{v_o}^{(j)}) \left(\dot{u}_\text{o} - \frac{U_\text{o}}{U} \dot{U} \right) + \cos(\gamma_{v_o}^{(j)}) \left(\dot{\beta}^{(j)} - \dot{\chi}_\text{o} \right) \right],$$

where

$$\dot{\beta}^{(j)} = \frac{U \sin(\gamma_\text{o} - \chi) - U_\text{o} \sin(\gamma_\text{o} - \chi_\text{o})}{R + d} \qquad (35)$$
$$\mp R \frac{U \cos(\gamma_\text{o} - \chi) - U_\text{o} \cos(\gamma_\text{o} - \chi_\text{o})}{(R + d) \sqrt{d(2R + d)}},$$

$$\dot{U} = Uv \frac{X r_\chi + Y v}{Xu + U^2}, \qquad (36)$$

and γ_o is the angle between the x-axis and the vehicle-obstacle line, as shown in Figure 4. Note that $\dot{\chi}_{\text{dca}}^{(j)}$ depends on r_χ. Inserting (34) into the course control law (12) gives

$$r_\chi = \frac{F_{\text{num}}}{F_{\text{den}}}, \qquad (37)$$
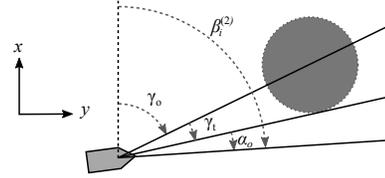

Fig. 4. Decomposition of $\beta^{(2)}$.

where

$$F_{\text{num}} \triangleq \dot{\beta}^{(j)} + \frac{1}{\sqrt{U^2 - U_o^2 \sin^2(\gamma_{v_o}^{(j)})}} \qquad (38)$$
$$\cdot \left[\sin(\gamma_{v_o}^{(j)}) \left(\dot{u}_\text{o} - \frac{U_\text{o} Y v^2}{U^2 + X u} \right) + \cos(\gamma_{v_o}^{(j)}) \left(\dot{\beta}^{(j)} - \dot{\chi}_\text{o} \right) - k_\chi \tilde{\chi} \right],$$

and

$$F_{\text{den}} \triangleq 1 + \frac{U_\text{o} \sin(\gamma_{v_o}^{(j)}) v X}{(U^2 + X u) \sqrt{U^2 - U_o^2 \sin^2(\gamma_{v_o}^{(j)})}}. \qquad (39)$$

Assumptions 3 and 5 ensure that (39) is well defined. In order for r_χ to be well defined, it is required that $F_{\text{den}} \neq 0$. Since $F_{\text{den}}(U_\text{o} = 0) = 1$, this can be ensured by requiring that F_{den} is lower bounded by a positive value. Minimizing with respect to $\gamma_{v_o}^{(j)}$ gives a lower bound of (39) as

$$F_{\text{den}} > 1 - \frac{U_{\text{o,max}} |v| |X|}{(U^2 + X u) \sqrt{U^2 - U_{\text{o,max}}^2}} := F_{\text{den,inf}}. \qquad (40)$$

Minimizing (40) with respect to v and solving for $U_{\text{o,max}}$ gives the following bound on $U_{\text{o,max}}$ to ensure that $F_{\text{den}} > 0$ for all $U_\text{o} \in [0, U_{\text{o,max}}]$:

$$U_{\text{o,max}} < \begin{cases} 2\sqrt{-X^2 - Xu} & -u < X \leq -\frac{u}{2} \\ u & -\frac{u}{2} < X. \end{cases} \qquad (41)$$

Assumption 5 ensures that (41) is satisfied.

When $d \geq d_{\text{safe}}$, a bound on $|F_{\text{num}}|$ can be found by using Assumptions 2 and 4-6:

$$|F_{\text{num}}| < \frac{v_{\text{sup}}^2 |Y| U_{\text{o,max}}}{U_{\text{d,sup}} \left(X + U_{\text{sup}}^2 \right)} + r_{\text{o,max}} \frac{U_{\text{o,max}}}{U_{\text{sup}}} \qquad (42)$$
$$+ \frac{a_{\text{o,max}}}{U_{\text{d,sup}}} + \frac{(U_{\text{sup}} + U_{\text{o,max}})^2}{d_{\text{safe}} U_{\text{sup}}} + k_\chi \pi := F_{\text{num,sup}}.$$

Equations (40) and (42) are symmetric in v_{sup}, hence

$$|r_\chi(\pm v_{\text{sup}})| < \frac{F_{\text{num,sup}}}{F_{\text{den,inf}}}. \qquad (43)$$

Inserting (43) into (24) bounds d_{safe} and k_χ to:

$$\frac{(U_{\text{sup}} + U_{\text{o,max}})^2}{d_{\text{safe}} U_{\text{sup}}} + k_\chi \pi \leq F_{kd}, \qquad (44)$$

where F_{kd} is given in (30). The design parameter σ can be used to rewrite (44) as

$$\frac{(U_{\text{sup}} + U_{\text{o,max}})^2}{d_{\text{safe}} U_{\text{sup}}} + k_\chi \pi \leq \sigma F_{kd} + (1 - \sigma) F_{kd}. \qquad (45)$$

Hence, conditions (31) and (32) ensure that (44), and thus (24), is satisfied. Lemma 1 then applies, and it follows that if $|v(0)| < v_{\sup}$, then $|v(t)| < v_{\sup} \; \forall t > 0$. ∎

In the next Lemma, we derive a bound on the minimum required switching distance d_{switch}.

Lemma 3: Consider a vehicle modeled by (4), controlled by (12) - (13). Let the vehicle enter CA mode at time t_1, with $d(t_1) = d_{\mathrm{switch}}$. Let Assumptions 1 and 5 hold, the vehicle speed satisfy $U < U_{\sup}$, and the switching distance satisfy

$$d_{\mathrm{switch}} \geq U_{\mathrm{o,max}} t_\epsilon + d_{\mathrm{safe}} + d_{\mathrm{turn}}, \qquad (46)$$

where

$$t_\epsilon \triangleq -\frac{\ln(\epsilon/\pi)}{k_\chi}, \quad \epsilon \in (0, \pi/2] \qquad (47)$$

and

$$d_{\mathrm{turn}} \triangleq \frac{U_{\sup}}{k_\chi} \mathrm{Si}(\frac{\pi}{2}). \qquad (48)$$

The function Si is the sine integral function, defined as

$$\mathrm{Si}(\tau) = \int_0^\tau \frac{\sin(\hat{\tau})}{\hat{\tau}} d\hat{\tau}. \qquad (49)$$

Then, the vehicle is able to converge to within ϵ rad of $\chi_{\mathrm{dca}}^{(j)}$ before the obstacle can be within d_{safe} of the vehicle.

Proof: Without loss of generality, let $x_{\mathrm{o}}(t_1) > x(t_1)$. Consider a worst case scenario where $R \to \infty$, so that the obstacle tangents are $\alpha^{(j)} = \pm \pi/2$, $j = 1, 2$, and let the vehicle and obstacle move at maximum speed towards each other: $U \to U_{\sup}$, $\chi(t_1) = 0$, $U_{\mathrm{o}} = U_{\mathrm{o,max}}$ and $\chi_{\mathrm{o}}(t_1) = \pi$. The worst case behavior of the obstacle is then to continue moving at maximum speed and course $\chi_{\mathrm{o}} = \pi$.

As the vehicle enters CA mode, it starts to turn towards $\chi_{\mathrm{dca}}^{(j)}$. Since $|\tilde{\chi}(0)| \leq \pi$ from the definition of $\tilde{\chi}$, and the course error dynamics is globally exponentially stable, the convergence time to $|\tilde{\chi}| \leq \epsilon$ is t_ϵ, given in (47). Hence, the distance covered by the obstacle towards the vehicle is upper bounded by $U_{\mathrm{o,max}} t_\epsilon$.

The distance traveled by the vehicle in the x direction before it has turned $\pm \pi/2$ rad is upper bounded by the distance traveled when making a $\pi/2$ turn. This can be found by solving (4a) when inserting $\tilde{\chi}(t) = -\frac{\pi}{2} e^{-k_\chi t}$:

$$\begin{aligned} &\int_0^\infty U_{\sup} \cos(\tilde{\chi} + \tfrac{\pi}{2}) dt \\ &= \int_0^\infty U_{\sup} \cos(\tfrac{\pi}{2} - \tfrac{\pi}{2} e^{-k_\chi t}) dt = \frac{U_{\sup}}{k_\chi} \mathrm{Si}(\frac{\pi}{2}). \end{aligned} \qquad (50)$$

It follows that if (46) holds, then the distance from the obstacle to the vehicle trajectory will not be less than d_{safe} before the vehicle course has converged to within ϵ rad of $\chi_{\mathrm{dca}}^{(j)}$, and this also holds for the distance d from the obstacle to the vehicle. ∎

The following assumption ensures that the target position is outside the circle of convergence around the obstacle:

Assumption 8: The distance $d_{\mathrm{o,t}}(t)$ from the obstacle to the target position p_{t} satisfies

$$d_{\mathrm{o,t}}(t) > \frac{R}{\cos(\alpha_{\mathrm{o}})} - R \qquad \forall t \geq 0. \qquad (51)$$

In addition, the must be able vehicle to start safely:
Assumption 9:

$$d(0) > d_{\mathrm{switch}}. \qquad (52)$$

We are now ready to state the main theorem:

Theorem 1: Let Assumptions 1-9 hold, the avoidance angle satisfy

$$\alpha_0 \in \left[\cos^{-1}\left(\frac{R}{R+d_{\mathrm{safe}}} \right) + \epsilon, \frac{\pi}{2} \right) \qquad (53)$$

and the switching distance satisfy

$$d_{\mathrm{switch}} \geq U_{\mathrm{o,max}} t_\epsilon + d_{\mathrm{safe}} + d_{\mathrm{turn}}. \qquad (54)$$

Furthermore, let the course control gain k_χ and safety distance d_{safe} satisfy the conditions of Lemma 2:

$$k_\chi \leq \frac{\sigma}{\pi} F_{kd}, \qquad (55)$$

$$d_{\mathrm{safe}} \geq \frac{(U_{\sup} + U_{\mathrm{o,max}})^2}{U_{\sup}} \frac{1}{(1-\sigma) F_{kd}}. \qquad (56)$$

Then a vehicle described by (1), controlled by (12) - (13), the guidance law (14) and the CA law (19) will maneuver to the target position p_{t} in the presence of an obstacle described by (6), while ensuring that

$$d(t) \geq d_{\mathrm{safe}} > 0 \quad \forall t \in [0, t_f], \qquad (57)$$

where t_f is the time of arrival at p_{t}

Proof:
It follows from Lemma 2 that v is bounded by

$$|v(t)| < v_{\sup} \quad \forall t \in [0, t_f]. \qquad (58)$$

Hence, the vehicle speed is bounded by $U < U_{\sup}$. Let the distance to the obstacle be reduced to d_{switch} at a time t_0, making the vehicle enter CA mode as described in Section IV-B. Lemma 3 then ensures that there is a time $t_1 > t_0$ when $d(t_1) >= d_{\mathrm{safe}}$ and $\chi(t_1) - \chi_{\mathrm{dca}}(t_1) \leq \epsilon$. Since $\tilde{\chi} = 0$ is an exponentially stable equilibrium, it is then assured that

$$\chi(t) - \chi_{\mathrm{dca}}(t) \leq \epsilon, \quad \forall t \in [t_1, t_2], \qquad (59)$$

where t_2 is the time when the vehicle will exit CA mode.

In a coordinate frame O moving with the obstacle velocity v_o the vehicle velocity is $v_\beta^{(j)}(t)$, defined in (15). Assumption 5 ensures that $u_\beta^{(j)} > 0$. Hence, the vehicle velocity in O maintains a constant angle α_0 to one of the tangents from the vehicle to the obstacle, as shown in Figure 2. The distance between the vehicle and the obstacle thus evolves as

$$\dot{d} = -u_\beta^{(j)} \cos(\gamma_{\mathrm{t}} + \alpha_0), \qquad (60)$$

where $\gamma_{\mathrm{t}} > 0$ is the angle from the line connecting the vehicle and the center of the obstacle to the tangent line, as seen in Figure 4. It follows that $\dot{d} < 0$ when $\gamma_{\mathrm{t}}(t) + \alpha_0 < \frac{\pi}{2}$, which occurs when $d > d_{\mathrm{min}}$. Furthermore, $\dot{d} > 0$ when $d < d_{\mathrm{min}}$ and $\dot{d} = 0$ when $d = d_{\mathrm{min}}$. Hence, the vehicle will converge to a circle $\mathcal{C}$ with center at the obstacle center and radius $\frac{R}{\cos(\alpha_0)}$, and (53) then gives

$$d(t) \geq d_{\mathrm{safe}} \quad \forall t \in [t_1, t_2], \qquad (61)$$

which satisfies control objective (10).

Since the vehicle circles around the obstacle, there will be a time t_2 when the line of sight to the target $\boldsymbol{p}_\mathrm{t}$ will be outside of $\mathcal{V}_\mathrm{c}$, and hence have a larger avoidance angle than α_o to $\mathcal{V}$. The vehicle will then exit CA mode and proceed towards the target.

A nearby obstacle may turn so that χ_dg comes within $\mathcal{V}_\mathrm{c}$ at a time when $d < d_\mathrm{switch}$, making the vehicle enter collision avoidance mode when (54) is not satisfied. However, since $\boldsymbol{v}_\mathrm{ca}^{(1)}$ and $\boldsymbol{v}_\mathrm{ca}^{(2)}$ are first order differentiable, and χ_dca is then chosen to be the closest of $\boldsymbol{v}_\mathrm{ca}^{(1)}$ and $\boldsymbol{v}_\mathrm{ca}^{(2)}$ by (23), the vehicle is immediately able to follow χ_dca to avoid the obstacle again.

Finally, since $u_\mathrm{max} > U_\mathrm{o,max}$, the vehicle will eventually escape the obstacle, and thus reach the target. The control objectives in Section II-D are thus met, which concludes the proof. ∎

VI. SIMULATIONS

In this section we present numerical simulations of an underactuated marine vehicle using the proposed collision avoidance algorithm. The simulated vehicle is a HUGIN autonomous underwater vehicle [21] operating in a horizontal plane. The vehicle surge speed is set to $u = 2\,\mathrm{m/s}$, and the maximum allowable sway speed is set to $v_\mathrm{sup} = 4\,\mathrm{m/s}$. It can be verified that Assumption 2 is satisfied with $Y = -1.10$, and that Assumption 3 is satisfied with $X = -1.59$.

The first scenario contains a circular obstacle with radius $R = 10\,\mathrm{m}$. The maximum obstacle speed is $U_\mathrm{o,max} = 1.35\,\mathrm{m/s}$, which satisfies Assumption 1. The obstacle keeps the maximum speed, and hence does not accelerate. The maximum turning rate is set to $r_\mathrm{o,max} = 0.25\,\mathrm{rad/s}$. The course control gain k_χ is set to 0.4, and the safety distance is set to $d_\mathrm{safe} = 10\,\mathrm{m}$, which satisfies the conditions of Lemma 2 with $\sigma = 0.62$. The convergence parameter ϵ is set to $\epsilon = 0.1\,\mathrm{rad}$. A lower bound on the avoidance angle is then given by (53) as $\alpha_\mathrm{o,min} = 1.15\,\mathrm{rad}$, while a minimum switching distance is given by (54) as $d_\mathrm{switch,min} = 37.0\,\mathrm{m}$. Both $\alpha_\mathrm{o,min}$ and $d_\mathrm{switch,min}$ are used in the simulation.

The vehicle and obstacle behavior in the first scenario is illustrated in Figure 5. The obstacle starts in front of the vehicle on a head on collision course, and is set to turn with the maximum turning rate towards the vehicle in order to pursue it. At time $8.39\,\mathrm{s}$ the vehicle reaches the switching distance d_switch from the obstacle, and enters collision avoidance mode in accordance with the switching rule in Section IV-B. Since the obstacle and vehicle is on a head on collision course, the choice of turning direction given in Section IV-C becomes random. In this case, the vehicle makes a starboard turn.

Figure 6 shows that $d > d_\mathrm{safe}$, even though the obstacle is in pursuit of the vehicle. Furthermore, the vehicle sway v is well within the designated v_sup. Hence, the simulation supports the theoretical results given by Theorem 1. At time $70.12\,\mathrm{s}$, the direction from the vehicle to the target comes outside the extended vision cone $\mathcal{V}_\mathrm{c}$, and following (22) the vehicle exits collision avoidance mode and enters
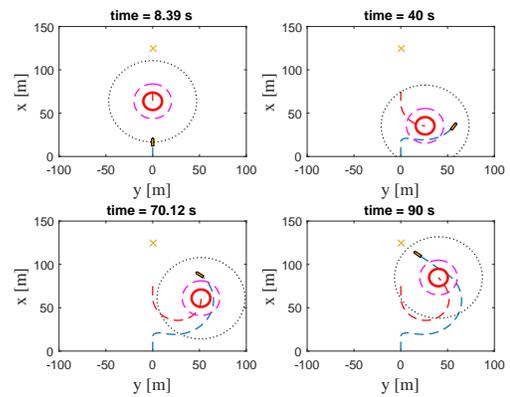
Fig. 5. The first scenario, with a circular obstacle in pursuit of the vehicle. The vehicle is shown in orange, while the obstacle is a solid red circle. The vehicle and obstacle trajectories are a dashed blue and a dashed red line, respectively. A dotted red circle shows d_safe, while d_switch is shown as a dotted black circle. The target position is marked by an 'X'.
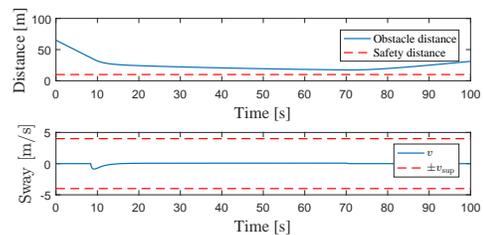
Fig. 6. Obstacle distance and vehicle sway in the second scenario.

guidance mode. It will then proceed towards the target using the pure pursuit guidance law (14).

The mathematical analysis in Section V only applies to circular obstacles. However, the proposed CA algorithm may also be applied to obstacles of a more general shape. This is demonstrated in the second scenario, where the obstacle has the shape of a ship that is $70\,\mathrm{m}$ long and $10\,\mathrm{m}$ wide. The simulation parameters are the same as in the first simulation. Figure 7 shows the behavior of system during the simulation, where the obstacle moves along a straight line from left to right, crossing in front of the vehicle.

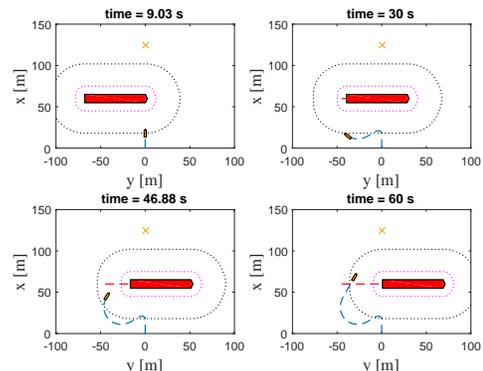Figure 8 shows that $d > d_\mathrm{safe}$ and $v < v_\mathrm{sup}$ during the

Fig. 7. The third scenario, where the obstacle has the shape of a ship.
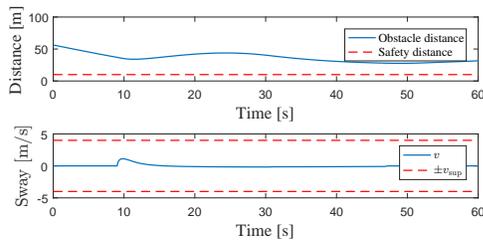
Fig. 8. Obstacle distance and vehicle sway in the third scenario.

maneuver. Note, however, that the analysis in Section V only applies for circular obstacles, or for obstacles modeled as a circular domain covering it. In this case, the covering domain would be quite large compared to the obstacle. Hence, the simulation demonstrates that a circular obstacle shape is a conservative requirement, and that the algorithm may also be applied to a non-circular obstacle.

VII. CONCLUSIONS

In this paper we have presented a reactive collision avoidance algorithm which avoids moving obstacles by keeping a constant avoidance angle between the vehicle velocity vector and the vision cone from the vehicle to the obstacle. In particular, we have considered marine vehicles with underactuated sway dynamics, where there is a component in the total vehicle speed that cannot be directly controlled. The proposed algorithm compensates for both the time-varying obstacle velocity and the underactuated sway motion. We have applied the algorithm to a vehicle with constant surge speed, and have thus shown its applicability to vehicles with high forward acceleration constraints. The proposed algorithm is intuitive, requires only limited obstacle measurements and has a low computational complexity.

The underactuated sway dynamics induce a sideways speed during turning, which can make the CA problem particularly challenging by driving the vehicle towards the obstacle. The proposed algorithm compensates for sway by steering the vehicle course, and we have shown that the sway motion is bounded during the maneuver. Furthermore, we have stated the conditions under which it is mathematically proved that the vehicle keeps at least a minimum safety distance to the obstacle. The theoretical results are supported by simulations, which also show that even though the analysis is concerned with circular obstacles only, the algorithm can also be applied to obstacles of a more general shape.

While we in this paper have assumed a single, circular obstacle in the analysis, the algorithm can also be used in scenarios with multiple obstacles of different shapes. Clustered obstacles will then be treated as one, making the vehicle move towards the outermost safe direction. However, a thorough analysis of scenarios with multiple obstacles remains the topic of future work.

ACKNOWLEDGMENT

REFERENCES

[1] K. Y. Pettersen and O. Egeland, "Exponential stabilization of an underactuated surface vessel," in *Proc. 35th IEEE Conference on Decision and Control*, (Kobe, Japan), pp. 1391–1396, 1991.

[2] T. Statheros, G. Howells, and K. M. Maier, "Autonomous Ship Collision Avoidance Navigation Concepts, Technologies and Techniques," *Journal of Navigation*, vol. 61, no. 01, pp. 129–142, 2008.

[3] C. Tam, R. Bucknall, and A. Greig, "Review of Collision Avoidance and Path Planning Methods for Ships in Close Range Encounters," *The Journal of Navigation*, vol. 62, no. 2009, pp. 455–476, 2009.

[4] M. Hoy, A. S. Matveev, and A. V. Savkin, "Algorithms for collision-free navigation of mobile robots in complex cluttered environments: a survey," *Robotica*, vol. 33, no. 03, pp. 463–497, 2014.

[5] O. Khatib, "Real-time obstacle avoidance for manipulators and mobile robots," *The International Journal of Robotics Research*, vol. 5, no. 1, pp. 90–98, 1986.

[6] Y. Koren and J. Borenstein, "Potential field methods and their inherent limitations for mobile robot navigation," in *Proc. IEEE International Conference on Robotics and Automation (ICRA)*, (Sacramento, CA, USA), pp. 1398–1404, 1991.

[7] J. Borenstein and Y. Koren, "The vector field histogram–Fast obstacle avoidance for mobile robots," *IEEE Transactions on Robotics and Automation*, vol. 7, no. 3, pp. 278–288, 1991.

[8] D. Fox, W. Burgard, and S. Thrun, "The dynamic window approach to collision avoidance," *IEEE Robotics and Automation Magazine*, vol. 4, no. 1, pp. 23–33, 1997.

[9] B. O. H. Eriksen, M. Breivik, K. Y. Pettersen, and M. S. Wiig, "A modified dynamic window algorithm for horizontal collision avoidance for AUVs," in *Proc. 2016 IEEE Conference on Control Applications (CCA)*, (Buenos Aires, Brazil), pp. 499–506, 2016.

[10] P. Fiorini and Z. Shiller, "Motion planning in dynamic environments using velocity obstacles," *The International Journal of Robotics Research*, vol. 17, no. 7, pp. 760–772, 1998.

[11] Y. Kuwata, M. T. Wolf, D. Zarzhitsky, and T. L. Huntsberger, "Safe maritime autonomous navigation with COLREGS, using velocity obstacles," *IEEE Journal of Oceanic Engineering*, vol. 39, no. 1, pp. 110–119, 2014.

[12] J. van den Berg, J. Snape, S. J. Guy, and D. Manocha, "Reciprocal collision avoidance with acceleration-velocity obstacles," in *Proc. IEEE International Conference on Robotics and Automation (ICRA 2011)*, (Shanghai, China), pp. 3475–3482, 2011.

[13] D. Wilkie, J. Van Den Berg, and D. Manocha, "Generalized velocity obstacles," in *Proc. IEEE/RSJ International Conference on Intelligent Robots and Systems,*, (St. Louis, MA, USA), pp. 5573–5578, 2009.

[14] E. J. Rodriguez-Seda, C. Tang, M. W. Spong, and D. M. Stipanovic, "Trajectory tracking with collision avoidance for nonholonomic vehicles with acceleration constraints and limited sensing," *The International Journal of Robotics Research*, vol. 33, pp. 1569–1592, Aug. 2014.

[15] S. Moe and K. Y. Pettersen, "Set-based Line-of-Sight (LOS) path following with collision avoidance for underactuated unmanned surface vessel," in *Proc. 24th Mediterranean Conference on Control and Automation (MED)*, (Athens, Greece), 2016.

[16] A. V. Savkin and C. Wang, "A simple biologically inspired algorithm for collision-free navigation of a unicycle-like robot in dynamic environments with moving obstacles," *Robotica*, vol. 31, no. 6, pp. 993–1001, 2013.

[17] M. S. Wiig, K. Y. Pettersen, and A. V. Savkin, "A reactive collision avoidance algorithm for nonholonomic vehicles," in *Proc. 1st IEEE Conference on Control Technology and Applications*, (Kona, HI, USA), 2017.

[18] T. I. Fossen, *Handbook of marine craft hydrodynamics and motion control*. John Wiley & Sons, 2011.

[19] E. Børhaug and K. Y. Pettersen, "LOS path following for underactuated underwater vehicle," in *Proc. 7th IFAC Conference on Manoeuvring and Control of Marine Craft*, (Lisbon, Portugal), 2006.

[20] M. Breivik and T. I. Fossen, "Guidance laws for planar motion control," in *Proceedings of the IEEE Conference on Decision and Control*, (Cancun, Mexico), pp. 570–577, 2008.

[21] P. E. Hagen, N. Storkersen, K. Vestgard, and P. Kartvedt, "The HUGIN 1000 autonomous underwater vehicle for military applications," in *Proc. Oceans 2003*, (San Diego, CA, USA), pp. 1141–1145, 2003.